Availability Analysis and Optimization in CoMP and CA-enabled HetNets

Jie Jia, *Member, IEEE*, Yansha Deng, *Member, IEEE*, Jian Chen, *Member, IEEE*, Abdol-Hamid Aghvami, *Fellow, IEEE*, and Arumugam Nallanathan, *Fellow, IEEE*

***Abstract*— Traditional cellular networks are moving toward heterogeneous cellular networks (HetNets) to satisfy the stringent demand for data rates and capacity. To enable the new applications in 5G, such as haptic communications, we face new challenges of achieving high availability with low latency in HetNets. In this paper, we introduce coordinated multi-point (CoMP) and carrier aggregation (CA) techniques in HetNets to guarantee the availability of all user equipment (UE), where the CoMP improves the single-path availability, and the CA enhances availability via multi-carrier gain combining. To characterize the availability, we first derive an exact closed-form expression for the availability of a random UE in a CoMP and CA-enabled HetNets. To achieve the maximum UE availability, we formulate a max–min optimization problem. To solve it, we then propose a two-step optimization algorithm (TSOA) and a joint (JTOA). The TSOA is based on heuristic algorithm for the optimal subcarrier assignment and UE association, and based on the Lagrangian dual method for the power allocation. The JTOA is based on genetic algorithm to achieve the interaction between the first step and the second step. Our results showcase the effective of our proposed JTOA, and the effective of the CoMP in availability improvement in HetNets.**

***Index Terms*— Heterogeneous cellular networks, high availability, coordinated multi-point, carrier aggregation, genetic algorithm.**

I. Introduction

IN THE past, cellular networks have mainly focused on achieving higher data rates and greater user capacities for human-centric applications, such as telephone, mobile internet or video streaming. However, it is expected that future wireless network will be complemented by a wide range of innovative and unconventional services and applications, such as M2M communication, IoT applications, machine-type communications (MTCs), and haptic communications. According to Gartner [2], about 6.4 billion connected things will be in use worldwide this year, which is nearly up to 30 percent increase from last year. And they also foretasted that the number would keep growing, and reach nearly 21 billion by the year 2020.

Usually, these specialized, mission-critical applications have specific requirements, which seems too stringent for the conventional human-centric applications, like the ultra high availability and ultra low latency requirements. Examples of application having these requirements include haptic communication [3], cloud computing [4], smart energy grids [5], vehicular communication [6], or factory automation [7]. The temporal availability requirement of these applications is 99.9999% (six nines) or higher. A more detailed example is that the factory automation application in a smart factory needs the end-to-end latency with 1ms and the availability requirement as 9 nines [8]. In other words, only one message in 10^9 data transfers can be lost or delayed in more than 1ms. A detailed analysis on future application as well as high availability requirement can be found in [9]. How to provide an availability of six nines or even higher for applications with ultra-reliable requirement using the existing or future cellular networks has become a major challenge.

The traditional cellular networks are undergoing a significant transition to handle the increasing wireless data demands, as well as the ever increasing availability requirement. Simply deploying more macro base stations (BSs) is no longer a sustainable solution to cope with those stringent requirements. Therefore, action is being taken to deploy more inexpensive, low-power, small-scale BSs, such as pico, femto BSs, underlaying the conventional cellular networks to improve the spectral efficiency and reduce the communication distance [10]. This is the so called heterogeneous cellular networks (HetNets). However, due to the heterogeneous deployments of those low power nodes, the interference management among tiers becomes very challenging and extremely important.

According to the reliability theory [11], there are two feasible methods to improve availability of a system: 1) the serial approach, which substitutes or adds more reliable sub-components in serial with the single sub-component system; and 2) the parallel approach, which enables multiple

Manuscript received August 31, 2016; revised December 30, 2016; accepted February 24, 2017. Date of publication March 8, 2017; date of current version June 14, 2017. This work is supported by the National Natural Science Foundation of China under Grant No. 61402096, No. 61173153 and No. 61572123; the Fundamental Research Funds for the Central Universities under Grant No. N150404006; the National Science Foundation for Distinguished Young Scholars of China under Grant No. 61225012 and No. 71325002; the Specialized Research Fund of the Doctoral Program of Higher Education for the Priority Development Areas under Grant No. 20120042130003. This paper was presented at the IEEE International Conference on Communications, Paris, 2017 [1]. The associate editor coordinating the review of this paper and approving it for publication was T. Q. S. Quek. *(Corresponding author: Yansha Deng.)*

J. Jia and J. Chen are with the Key Laboratory of Medical Image Computing of Northeastern University, Ministry of Education, Shenyang 110819, China, and also with the School of Computer Science and Engineering, Northeastern University, Shenyang 110819, China, and also with the Department of Informatics, King's College London, London WC2R 2LS, U.K. (e-mail: jiajie@mail.neu.edu.cn; chenjian@mail.neu.edu.cn).

Y. Deng, A.-H. Aghvami, and A. Nallanathan are with the Department of Informatics, King's College London, London WC2R 2LS, U.K. (e-mail: yansha.deng@kcl.ac.uk; hamid.aghvami@kcl.ac.uk; arumugam.nallanathan@kcl.ac.uk).

Color versions of one or more of the figures in this paper are available online at http://ieeexplore.ieee.org.

Digital Object Identifier 10.1109/TCOMM.2017.2679747

sub-components working in parallel. Multi-connection is one example using parallel approach, where the receiver is allowed to be served by multiple transmitters simultaneously, in order to achieve the multi-link diversity gain and availability improvement [12]–[16].

In [12], it was shown that the higher availability could be achieved via multiple less reliable links connection than single powerful link connection. However, this work was limited to Rayleigh-fading links. The model in [12] has been extended to [13] by including selection combining and maximal ratio combining over Nakagami-m fading. In [14], combined macro- and uplink connections was studied under Nakagami fading and log-normal shadowing. In [15], multi-input multi-output (MIMO) was proposed to achieve ultra-reliable and low-latency communications in 5G machine-type communication (MTC) use cases. It is noticed that [12]–[15] only considered the single-user case, and hence the effects resulted from multi-user and multi-cell interference are not explicitly studied [16].

Due to the different achievable capacity of each link and cumulative interference caused by all the simultaneously transmitting nodes, nearby or faraway [17], simply considering the received power from the desired transmitter may not accurately capture the availability characteristics. A more appropriate model is to measure the signal quality in terms of the signal-to-interference-plus-noise ratio (SINR) value. The SINR is, however, affected by many variable factors that are intrinsic for any wireless systems. The desired signal power can be slightly attenuated as a result of the fading nature of the wireless channel, whereas the received interference can be large due to the typical aggressive reuse of the time-frequency resources for maximizing the system capacity in the network. Assuming the shadowing fading as a random variable, [18] studied the high availability in wireless networks with different transmit power at the BS based on SINR model. However, modeling and analyzing the availability in HetNets based on SINR model can be computationally and analytically challenging.

Another example of multi-connectivity is the carrier aggregation (CA) technique [19], where the concurrent utilization of multiple component carriers (CCs) at the physical layer is enabled, bringing wider effective bandwidth. CA has already been included in the 3rd Generation Partnership Project (3GPP), which combines contiguous or non-contiguous spectrum fragments to create a virtual wideband channel. The aggregated bandwidth as large as 100MHz can be obtained by aggregating 5 20MHz CCs, and the propagation characteristics of different component carriers may also vary significantly. e.g., a CC in the 800MHz has very different propagation characteristic from a CC in the 2.4 GHz. With CA, another dimension of diversity can be achieved via carrier-selecting fading [20].

Even though CA improves the availability of single user equipment (UE) in HetNets via multi-path connectivity, the single path availability is still low due to the full spectrum reuse in HetNets [21], [22]. The intercell interference is the most detrimental factor impairing the single path availability. To cope with it, coordinated multi-point (CoMP) was proposed in 3GPP [23]. With CoMP, the BSs in coordinated BS cluster are connected via a backhaul link, and transmit data to the UE simultaneously to improve single path availability under universal frequency reuse [24].

Different from CA that exploiting the spectral diversity gain, CoMP is a coordination technique between BSs to enhance inter-cell interference coordination in the same carrier. There are two categories of CoMP: 1) CoMP coordinated beamforming (CoMP-CB) was proposed to avoid inter-cell interference [25]; and 2) CoMP joint processing (CoMP-JP) is capable of converting the inter-cell interference to useful signal [26], therefore provides an external capacity gain over CoMP-CB. More importantly, with the help of CoMP-JP, the availability gain of each path can be achieved to bring substantial overall availability improvement of single UE [27]. However, their potential to provide ultra-reliable communications in HetNets has not been treated until recently.

The resource allocation is an effective way to optimize the system performance for cellular networks with CA/CoMP. In [20], the joint downlink and uplink resource allocation for energy-efficient CA was studied, where the optimal power allocation was solved using the Lagrangian dual method. In [28], a joint clustering and resource allocation problem for ultra dense cellular networks was solved using a two-step algorithm, which consists of the user-centric clustering based on load information and scheduling algorithm based on graphic coloring. In [29], the subcarrier allocation algorithm was proposed to satisfy both throughput and fairness. In [30], with the aim of maximizing the energy efficiency, the joint optimization on BS coordination, user scheduling, data rate adaption, and power allocation was solved via iterative algorithm.

Different from aforementioned works, the aim of this work is to achieve high UE availability in HetNets with the help of CA and CoMP. To the best of our knowledge, this is the first work taking into account the SINR-based availability modeling and optimization in HetNets. The main contributions of this paper are summarized as follows:

- We propose CoMP and CA-enabled HetNets to improve the UE availability in HetNets, where CoMP improves the availability of each path via interference coordination, and CA improves the UE availability via multi-carrier gain combining. This approach for availability improvement is different from previous works only using parallel method [12], [13].
- We present an analytical model for the UE availability in CoMP and CA-enabled HetNets based on SINR model. Different from the coverage model or outage model defined in [31] and [32], where a UE connects to one BS offering the highest instantaneous SINR, we assume each UE can be served by multiple subcarriers and multiple BSs via muli-path connectivity.
- We derive an exact closed-form expression for the availability of a random UE in CoMP and CA-enabled HetNets, which is verified by Monte Carlo simulation. Its numerical results reveal the importance of the UE association, the subcarrier assignment and the power allocation in achieving high availability.

- We formulate an optimization problem with the aims of maximizing the minimum UE availability for multi users under the BS transmit power constraint in a multi-cell HetNet. Due to the complex topology of proposed model, the optimization problem is NP-hard in nature.
- We first propose the two-step optimization algorithm (TSOA) to solve the optimization problem. In this algorithm, the optimal subcarrier assignment and UE association is determined first via heuristic algorithm under equal power allocation, and the optimal power allocation is obtained via Lagrangian dual based method with the predetermined optimal subcarrier assignment.
- We then propose the joint two-step optimization algorithm (JTOA), which is an integration of the TSOA with the GA algorithm to achieve the interaction between the first step and the second step. Numerical results show that our JTOA is an effective way for availability improvement.

The remainder of this paper is organized as follows. In Section II, we present the multi-tier multi-band availability model. Next, in Section III, we formulate the availability optimization problem. In section IV, we propose the TSOA and JTOA. Section V presents the numerical results and Section VI highlights our conclusions.

II. System Model

A. Availability Analysis

We consider HetNets including macrocells, picocells, femtocells, and further radiating elements. In this network, there are N randomly distributed UEs, denoted as $\mathcal{N} = \{1, 2, \ldots, N\}$, and the set of BSs as $\mathcal{B} = \{1, 2, \ldots, S\}$, where S represents the number of BSs. Each BS has Q available bands (e.g., 800MHz, 2.4GHz, ...), each spectrum band contains F orthogonal subcarriers. We denote the set of bands in each BS as $\mathcal{Q} = \{1, 2, \ldots, Q\}$, and the set of subcarriers at each BS as $\mathcal{M} = \{\underbrace{1, \ldots, F}_{band_1}, \ldots, \underbrace{(Q-1)F+1, \ldots, QF}_{band_Q}\}$. We focus on the downlink transmission with open access for all the small cells.

With CoMP, the coordinated BS cluster can transmit data to the UE simultaneously to eliminate the co-channel interference and improve the received signal quality. The BSs in each coordinated BS cluster are connected via high-capacity backhaul links on which complex signaling and user data are exchanged [33]. To fully exploit the macro diversity of coordinated BS cluster, we adopt the user-centric adaptive clustering [34], where any UEs can be served by arbitrary number of coordinated BSs, and the coordinated BS cluster for each UE can overlap with each other. Each UE can access to different sub-carriers in each BS simultaneously, and can potentially aggregate data from all the available sub-carriers. For clarify, Fig. 1 presents the illustration of our system model with 3 BSs and 2 UEs, where each UE can aggregate 2 sub-carriers, and each UE can also apply CoMP technique on one sub-carrier to enhance its availability.

To specify the UE association and the resource assignment, we denote $\upsilon_{s,n}^m$ as the resource-allocation indicator binary variable. If $\upsilon_{s,n}^m = 1$, it indicates that the mth subcarrier of the sth BS ($s \in \mathcal{B}$) is allocated to the nth UE ($n \in \mathcal{N}$), and if otherwise $\upsilon_{s,n}^m = 0$ ($m \in \mathcal{M}$). To specify the power allocation, we denote the power allocated at the mth subcarrier of the sth BS is $P_{s,m}$, where

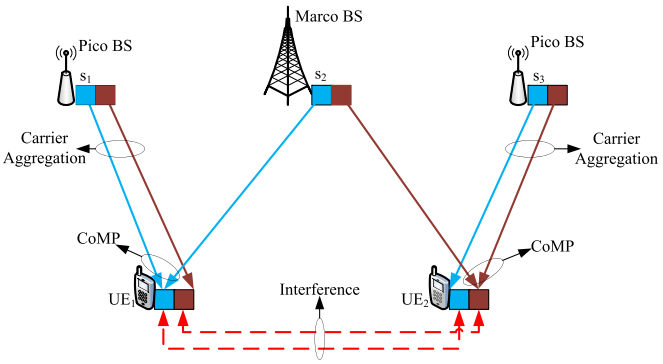

Fig. 1. System model with CoMP and CA.

$$P_{s,m} \begin{cases} \in (0, P_s^{\max}], \text{If UE occupied } m\text{th subcarrier of } s\text{th BS}, \\ = 0, \text{If no UE occupied } m\text{th subcarrier of } s\text{th BS}, \end{cases} \tag{1}$$

and $P_s^{\max}$ is the maximum transmit power of the sth BS.

Due to the hardware limitation, the following per-subcarrier assignment constraint and per BS power constraint need to be satisfied:

1) The variable $\upsilon_{s,n}^m$ must satisfy that each subcarrier for a BS can only be occupied by at most one UE.

2) The total transmit power at each BS over all its sub-carriers $\sum_m P_{s,m}$ should not exceed its maximum power P_s^{max}.

We define the set of coordinated BS cluster serving the nth UE at the mth sub-carrier as $\mathcal{B}_n^m = \{s | \upsilon_{s,n}^m = 1, s \in \mathcal{B}, m \in \mathcal{M}\}$, the SINR of the nth UE at the mth subcarrier with CoMP-JP is formulated as

$$SINR_n^m = \frac{\sum\limits_{i \in \mathcal{B}_n^m} P_{i,m} H_{i,n} C_q d_{i,n}^{-\alpha_q}}{\underbrace{\sum\limits_{j \in \mathcal{B} - \mathcal{B}_n^m} P_{j,m} H_{j,n} C_q d_{j,n}^{-\alpha_q} + N_0}_{I_n^m}}, \tag{2}$$

where $q = \lceil m/F \rceil$, with $\lceil \cdot \rceil$ as the ceiling function, I_n^m is the aggregate interference at the nth UE from all the other non-coordinated BSs, α_q is the path loss exponent of the qth band, $H_{i,n}$ is the random variable capturing the fading effects of the subcarrier between the ith BS and the nth UE, $d_{i,n}$ is the distance between the ith BS and the nth UE, N_0 is the noise power, and C_q is the constant depends strongly on carrier frequency with $C_q = (\frac{\mu_q}{4\pi})^2$ for the wavelength μ_q. Similar as [22], we ignore shadowing and only consider Rayleigh fading with $H_{i,n} \sim \exp(1)$ for simplicity.

According to the user-centric adaptive clustering, the choices and the size of coordinated BS cluster for each UE can be adaptive. It can be seen from (2) that increasing the number

of BSs in the coordinated BS cluster for a given UE increases its SINR value, due to that the coordinated BS cluster convert the intercell interference between each other to the useful signal. However, it should be also be noted that increases the number of BSs involved in this coordinated BS cluster decreases the probability of other UEs accessibility, due to the fact that all sub-carriers in a cell are orthogonal and each sub-carrier can only be occupied by at most one UE at a time.

The signal of a single path cannot be successfully received if the SINR value $SINR_n^m$ is below a certain threshold τ, thus the availability of the nth UE associated with the coordinated BS cluster $\mathcal{B}_n^m$ at the mth subcarrier is expressed as

$$A_n^m = \mathcal{P}\left(SINR_n^m > \tau\right). \tag{3}$$

And the availability nth UE in HetNets is defined by the combination of multiple single-path availabilities (parallel model), which is derived in the following theorem.

Theorem 1: The availability of the nth UE in a HetNet with CoMP-JP and CA is derived as

$$A_n = 1 - \prod_{m\in\mathcal{M}} \left(1 - A_n^m\right), \quad \forall n \in \mathcal{N}, \tag{4}$$

where

$$A_n^m = \begin{cases} 0 & \text{if } B_n^m = \emptyset \\ \Omega_{\mathcal{B}_n^m} \sum\limits_{s\in\mathcal{B}_n^m} \dfrac{e^{-\Xi_s \tau N_0}}{\Theta_{\mathcal{B}_n^m/s}} & \text{if } B_n^m \neq \emptyset, I_n^m = 0 \\ \Omega_{\mathcal{B}} \sum\limits_{s\in\mathcal{B}_n^m} \sum\limits_{j\in\mathcal{B}-\mathcal{B}_n^m} \dfrac{e^{-\Xi_s N_0 \tau}}{(\Xi_j + \Xi_s\tau)\Theta_{\mathcal{B}-\mathcal{B}_n^m/j}\Theta_{\mathcal{B}_n^m/s}} & \text{if } B_n^m \neq \emptyset, I_n^m \neq 0 \end{cases} \tag{5}$$

with

$$\Xi_s = \frac{1}{P_{s,m} C_q d_{s,n}^{-\alpha_q}}. \tag{6}$$

$$\Omega_{\mathcal{B}_n^m} = \prod_{i\in\mathcal{B}_n^m/s} \Xi_i, \tag{7}$$

$$\Omega_{\mathcal{B}} = \prod_{i\in\mathcal{B}/s} \Xi_i \tag{8}$$

$$\Theta_{\mathcal{B}_n^m/s} = \prod_{k\in\mathcal{B}_n^m/s} \left(\Xi_k - \Xi_s\right), \tag{9}$$

and

$$\Theta_{\mathcal{B}-\mathcal{B}_n^m/j} = \prod_{l\in\mathcal{B}-\mathcal{B}_n^m/j} \left(\Xi_l - \Xi_j\right). \tag{10}$$

Proof: For $B_n^m = \emptyset$, we can directly obtain $A_n^m = 0$.

For the case $B_n^m \neq \emptyset$ and with no interference $I_n^m = 0$, we have

$$\begin{aligned} A_n^m &= \mathcal{P}\left(SINR_n^m > \tau\right) \\ &= \mathcal{P}\Big(\sum_{s\in\mathcal{B}_n^m} \frac{1}{\Xi_s} H_{s,n} \geq \tau N_0\Big). \end{aligned} \tag{11}$$

In order to obtain the probability density function (PDF) of $Y = \sum\limits_{s\in\mathcal{B}_n^m} \frac{1}{\Xi_s} H_{s,n}$, we apply the lemma as follows [35].

Lemma 1: Let $(X_i)_{i=1\ldots n}$, $n \geq 2$, be independent exponential random variables with pairwise distinct respective parameters θ_i. we have the PDF of their sum as

$$f_{X_1+X_2+\ldots+X_n}(X) = \Big(\prod_{i=1}^{n} \theta_i\Big) \sum_{i=1}^{n} \frac{e^{-\theta_i x}}{\prod\limits_{k=1,k\neq i}^{n} (\theta_k - \theta_i)}. \tag{12}$$

Based on Lemma 1, the PDF of $Y = \sum_{s\in\mathcal{B}_n^m} \frac{1}{\Xi_s} H_{s,n}$ is derived as

$$f_Y(y) = \Big(\prod_{i\in\mathcal{B}_n^m} \Xi_i\Big) \sum_{s\in\mathcal{B}_n^m} \frac{e^{-\Xi_s y}}{\prod\limits_{k\in\mathcal{B}_n^m/s} \left(\Xi_k - \Xi_s\right)}. \tag{13}$$

Substituting (9) into (7), we obtain

$$\begin{aligned} A_n^m &= \mathcal{P}\left(SINR_n^m > \tau\right) \\ &= \int_{\tau N_0}^{\infty} f_Y(y)\, dy \\ &= \Big(\prod_{i\in\mathcal{B}_n^m} \Xi_i\Big) \sum_{s\in\mathcal{B}_n^m} \frac{e^{-\Xi_s \tau N_0}}{\Xi_s \prod\limits_{k\in\mathcal{B}_n^m/s} \left(\Xi_k - \Xi_s\right)} \\ &= \Big(\prod_{i\in\mathcal{B}_n^m/s} \Xi_i\Big) \sum_{s\in\mathcal{B}_n^m} \frac{e^{-\Xi_s \tau N_0}}{\prod\limits_{k\in\mathcal{B}_n^m/s} \left(\Xi_k - \Xi_s\right)}. \end{aligned} \tag{14}$$

For $\mathcal{B}_n^m \neq \phi$ and $I_n^m \neq 0$, we employ the change of variables $X = I_n^m + N_0$ and $Z = Y/X$ to obtain

$$\begin{aligned} A_n^m &= \mathcal{P}(z > \tau) \\ &= \int_{\tau}^{\infty} f_Z(z)\, dz \\ &= \int_{\tau}^{\infty} \int_{0}^{\infty} x f_X(x) f_Y(xz)\, dx dz. \end{aligned} \tag{15}$$

By plugging $y = xz$ into (14), we obtain

$$f_Y(xz) = \Big(\prod_{i\in\mathcal{B}_n^m} \Xi_i\Big) \sum_{s\in\mathcal{B}_n^m} \frac{e^{-\Xi_s xz}}{\prod\limits_{k\in\mathcal{B}_n^m/s} \left(\Xi_k - \Xi_s\right)}. \tag{16}$$

Next, we focus on computing $f_x(x)$. Employing $t_i = \frac{l_{i,m}}{L} P_{i,m}^{\max} H_{i,n} C_m d_{i,n}^{-\alpha_q}$ and $t = I_n^m$, we can rewrite t as

$$t = \sum\nolimits_{i\in B-B_n^m} t_i, \tag{17}$$

with

$$f_{t_i}(x) \sim \Xi_i exp\left(-\Xi_i x\right), \tag{18}$$

where $\Xi_i = \frac{1}{P_{i,m} C_q d_{i,n}^{-\alpha_q}}$.

Based on Lemma 1, the PDF of $\sum\limits_{i\in B-B_n^m} t_i$ is derived as

$$\begin{aligned} f_X(x) &= f_{I_n^m}(x - N_0) \\ &= \prod_{j\in\mathcal{B}-\mathcal{B}_n^m} \Xi_j \sum_{j\in\mathcal{B}-\mathcal{B}_n^m} \frac{e^{\Xi_j N_0}}{\prod\limits_{l\in\mathcal{B}-\mathcal{B}_n^m/j} \left(\Xi_l - \Xi_j\right)} e^{-\Xi_j x}. \end{aligned} \tag{19}$$

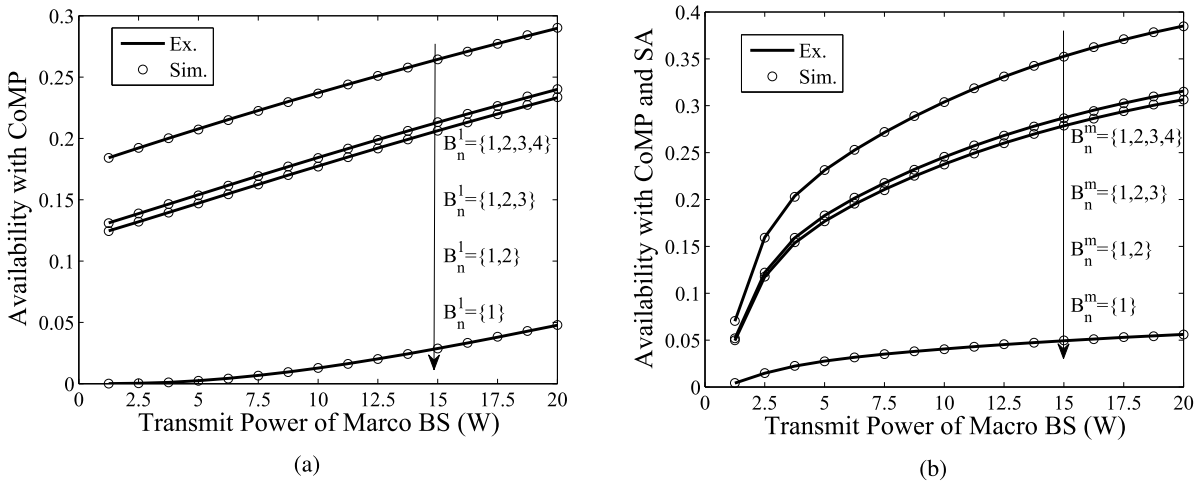

Fig. 2. (a) Single UE Availability with CoMP, (b) Single UE Availability with CoMP and CA.

Combining (15), (16) and (19), we obtain

$$A_n^m = \prod_{i\in\mathcal{B}} \Xi_i \sum_{s\in\mathcal{B}_n^m} \sum_{j\in\mathcal{B}-\mathcal{B}_n^m} \frac{e^{\Xi_j N_0}}{\prod_{k\in\mathcal{B}_n^m/s}(\Xi_k-\Xi_s)} \frac{Z\left(\tau, N_0, \theta_j+\theta_s z\right)}{\prod_{l\in\mathcal{B}-\mathcal{B}_n^m/j}\left(\Xi_l-\Xi_j\right)}, \tag{20}$$

where

$$\begin{aligned} &Z\left(\tau, N_0, \Xi_j+\Xi_s z\right) \\ &= \int_\tau^\infty \int_{N_0}^\infty x e^{-\left(\Xi_j+\Xi_s z\right)x} dx dz \\ &= \int_\tau^\infty \left(\frac{N_0 \mathrm{e}^{-N_0\left(\Xi_j+\Xi_s z\right)}}{\left(\Xi_j+\Xi_s z\right)} + \frac{\mathrm{e}^{-N_0\left(\Xi_j+\Xi_s z\right)}}{\left(\Xi_j+\Xi_s z\right)^2}\right) dz. \end{aligned} \tag{21}$$

Employing a change of variable of $u = N_0\left(\Xi_j+\Xi_s z\right)$, we obtain

$$\begin{aligned} &Z\left(\tau, N_0, \Xi_j+\Xi_s z\right) \\ &= \int_{N_0\left(\Xi_j+\Xi_s\tau\right)}^\infty \left(\frac{N_0}{\Xi_s}\frac{\mathrm{e}^{-u}}{u} + \frac{N_0}{\Xi_s}\frac{\mathrm{e}^{-u}}{u^2}\right) du \\ &= \frac{\mathrm{e}^{-N_0\left(\Xi_j+\Xi_s\tau\right)}}{\Xi_s\left(\Xi_j+\Xi_s\tau\right)}. \end{aligned} \tag{22}$$

Combining (20) and (22), we obtain A_n^m with $B_n^m \neq \phi$ and $I_n^m \neq 0$ as

$$\begin{aligned} A_n^m = &\prod_{i\in\mathcal{B}/s} \Xi_i \sum_{s\in\mathcal{B}_n^m} \sum_{j\in\mathcal{B}-\mathcal{B}_n^m} \frac{1}{\prod_{k\in\mathcal{B}_n^m/s}\left(\Xi_k-\Xi_s\right)} \\ &\times \frac{e^{-\Xi_s N_0\tau}}{\left(\Xi_j+\Xi_s\tau\right)\prod_{l\in\mathcal{B}-\mathcal{B}_n^m/j}\left(\Xi_l-\Xi_j\right)}. \end{aligned} \tag{23}$$

■

B. Availability Validation

To verify the derived analytical results, we plot the analytical curves for the availability with CoMP-JP and the availability with CoMP-JP and CA using (23) and (4) with the simulation points using Monte Carlo simulation in Fig. 2a and Fig. 2b, where Ex. denotes the Exact results from (4) and Sim. denotes the results from Monte Carlo Simulation. In these two figures, we consider two-tier HetNets, including single macro BS with $P_{j,m}$ = 46 dBm, 4 pico BSs with $P_{j,m}$ = 30 dBm, and single UE. The single UE and all these BSs are randomly deployed in a circle area with radius of 500m, and the path loss exponent is set as 4. Both figures demonstrate the well match between the derived analytical results and the simulation, which proves the accuracy of our derived results.

In Fig. 2a, we plot the availability of the single UE versus the transmit power at the macro BS with different number of BSs in the coordinated BS cluster $\mathcal{B}_n^1$, with the single subcarrier in each BS ($M = 1$). In Fig. 2b, we plot the availability of the single UE with CA, where the number of subcarriers at each BS is $M = 2$ with $C_{q_1} = (\frac{0.375}{4\pi})^2$, and $C_{q_2} = (\frac{0.125}{4\pi})^2$, respectively. The equal power allocation is applied in each subcarrier, Note that the CoMP-JP technique is not used when $\mathcal{B}_n^m = \{1\}$ in both figures.

We first observe that the availability of the single UE increases with increasing the transmit power at the macro BS and the number of coordinated BSs. However, due to the uneven distribution of these BSs, the distance between the UE and BSs are not equal, and the improvement gap between $B_n^m = \{1, 2\}$ and $B_n^m = \{1\}$ is larger than that between with $B_n^m = \{1, 2, 3\}$ and $B_n^m = \{1, 2\}$, which also reveals the importance of UE association for availability improvement. Comparing Fig. 2a with Fig. 2b, we see that the availability of the single UE occupying two subcarriers substantially outperforms that occupying single subcarrier, which reveals the benefits of CA technique. However, due to the interference from the non-coordinated BSs, the availability in Fig. 2b is still far from the availability goal of six nines, which reveals the importance of using resource allocation to optimize the availability.

III. Problem Formulation

The target of this paper is to maximize the minimum availability among all UEs, which is referred to the

Max-Min Availability optimization problem. To achieve this, an optimization algorithm is required to perform the optimal UE association, resource assignment, and power allocation under the transmit power constraint of each BS. We first present the optimization problem as

$$\max_{\boldsymbol{v},\boldsymbol{P}} \ \min_{n} A_n \tag{24}$$

$$\text{s.t.} \ \sum\nolimits_{m} P_{s,m} \le P_s^{max}, \quad \forall s \in \mathcal{B}, \tag{25a}$$

$$\sum\nolimits_{n\in\mathcal{N}} v_{s,n}^m \le 1, \quad \forall s \in \mathcal{B}, \ \forall m \in \mathcal{M}, \tag{25b}$$

$$P_{s,m} \ge 0, \quad \forall s \in \mathcal{B}, \ \forall m \in \mathcal{M}, \tag{25c}$$

$$v_{s,n}^m \in \{0,1\}, \quad \forall n \in \mathcal{N}, \ \forall m \in \mathcal{M}, \ \forall s \in \mathcal{B}. \tag{25d}$$

In (24), A_n is given by (4). The constraint in (25a) indicates that the maximum power constraint of each BS, and the constraints (25b) indicates that each BS can be allocated to at most one UE. Relying on the strictly increasing characteristic of logarithmic function [36], we thus convert the optimization problem of (24) into the following equivalent problem

$$\min_{\boldsymbol{v},\boldsymbol{P}} \ \max_{n} \sum\nolimits_{m} \ln\left(1 - A_n^m\right) \tag{26}$$

$$\text{s.t.} \ \sum\nolimits_{m} P_{s,m} \le P_s^{max}, \quad \forall s \in \mathcal{B}, \tag{27a}$$

$$\sum\nolimits_{n\in\mathcal{N}} v_{s,n}^m \le 1, \quad \forall s \in \mathcal{B}, \ \forall m \in \mathcal{M}, \tag{27b}$$

$$P_{s,m} \ge 0, \quad \forall s \in \mathcal{B}, \ \forall m \in \mathcal{M}, \tag{27c}$$

$$v_{s,n}^m \in \{0,1\}, \quad \forall n \in \mathcal{N}, \ \forall m \in \mathcal{M}, \ \forall s \in \mathcal{B}. \tag{27d}$$

Optimizing $v_{s,n}^m$ and $P_{s,m}$ in (26) is a mixed integer programming problem, which is generally NP-hard, so the optimality for any polynomial time solutions is hard to guarantee. However, if we relax the integer constraint ($v_{s,n}^m \in \{0,1\}$) by treating $v_{s,n}^m$ as a sharing factor ($0 \le v_{s,n}^m \le 1$), or determine $v_{s,n}^m$ by some other method, the optimization problem becomes a convex optimization problem, because the objective function is concave and all constraints are linear [37]. Remind that simply relaxing $v_{s,n}^m$ may results in non-integer solutions of subcarrier assignment. To avoid that, we propose the two-step optimization algorithm, where the optimal subcarrier assignment and UE association achieving (24) with equal power allocation is determined and fixed first, and then the optimal power allocation is obtained using Lagrangian dual based method.

IV. Optimization Algorithms

In this section, we propose two optimization algorithms to solve the max-min optimization problem: the TSOA and the JTOA. In both algorithms, we divide the resource allocation into the power allocation, and the subcarrier assignment and UE association. In TSOA, the optimal subcarrier assignment and UE association is determined first via heuristic algorithm under equal power allocation, and the optimal power allocation is obtained via Lagrangian dual based method with the predetermined optimal subcarrier assignment. The JTOA is an integration of the two-step optimization algorithm with the GA algorithm to achieve the interaction between the first step and the second step. In this algorithm, the optimal subcarrier assignment and UE association is obtained by GA, and the Lagrangian based power allocation is used to evaluate the fitness of each individual in GA and guide the evolution process.

Algorithm 1 Heuristic Algorithm for Subcarrier Assignment and UE Association

Initialization
Set $A_n^m = 0$, $v_{s,n}^m = 0$, and $P_{s,m} = \frac{P_s^{max}}{M}$ for $\forall n \in \mathcal{N}, \forall s \in \mathcal{B}, \forall m \in \mathcal{M}$
Set $\mathcal{F} = \{\mathcal{F}_1, \mathcal{F}_2, \cdots, \mathcal{F}_S\}$, and $\mathcal{F}_s = \{1, 2, \cdots, M\}$
$Counter = S \times M$
while $\mathcal{F} \neq \emptyset$ **do**
  Step1: UE selection
  Find UE n^* satisfies $A_{n^*} < A_k \ \forall k \in \mathcal{N}$
  Step2: potential gain calculation
  for $s = 1$ **to** B **do**
    for $m \in \mathcal{F}_s$ **do**
      Calculate and record $G_{s,n^*}^m = Cur(A_{n*}^m) - Pre(A_{n*}^m)$
    end
  end
  Step3: subcarrier assignment
  Find a subcarrier m^* in BS s^* satisfies $G_{s^*,n^*}^{m^*} > G_{s,n^*}^m$ $\forall m \in \mathcal{F}_s, \forall s \in \mathcal{B}$
  Update $v_{s^*,n^*}^{m^*} = 1$, $\mathcal{F}_{s^*} = \mathcal{F}_{s^*}/m^*$, and $\mathcal{F} = \mathcal{F}/m^*$
end

A. Two-Step Optimization Algorithm

In this subsection, we present the first step and the second step of TSOA in the following subsections.

1) Subcarrier Assignment and UE Association: In this section, we propose the heuristic algorithm for sub-carrier assignment to decide $\{v_{s,n}^m\}$. The description of **Algorithm 1** for the subcarrier assignment and UE association is given in the following.

In the initialization step of **Algorithm 1**, we assume the equal power allocation among all BSs and thus the power allocation vector at any subcarrier of each BS is given as $P_{s,m} = \frac{P_s^{max}}{M}$. We denote $\mathcal{F}_s = \{1, 2, \cdots, M\}$ as the available subcarrier set of the sth BS, and $\mathcal{F} = \{\mathcal{F}_1, \mathcal{F}_2, \cdots, \mathcal{F}_S\}$ as all the available subcarriers of all BSs with the total number of the available subcarriers as $|\mathcal{F}| = S \times M$ during the initialization.

After the initialization, the heuristic algorithm performs three steps: *the UE selection*, *the potential gain calculation* and *the subcarrier assignment*. At *the UE selection* step, the UE with the lowest availability n^* is selected as the first to be given access to subcarrier, with the objective of maximizing the minimum availability among UEs as in (24). If there are more than one UEs with the same minimum availability, a random UE among them is selected.

At *the potential gain calculation* step, we calculate the potential availability gain before and after single subcarrier m is allocated to UE n^*. For an available subcarrier $m \in \mathcal{F}_s$, we denote $Pre(A_{n^*}^m)$ and $Cur(A_{n^*}^m)$ as the availability of UE n^* before and after $m \in \mathcal{F}_s$ is allocated to UE n^*, respectively. Thus, the potential gain G_{s,n^*}^m for allocating mth subcarrier

of sth BS to n^* UE is given by

$$G^m_{s,n^*} = Cur(A^m_{n^*}) - Pre(A^m_{n^*}). \tag{28}$$

Using (28), we calculate and record the potential gains G^m_{s,n^*} for all the available subcarriers and all the available BSs. At *the subcarrier assignment* step, the optimal subcarrier m^* of the BS s^* with the maximum potential gain $G^{m^*}_{s^*,n^*}$ is assigned to the n^*th UE. Note that only single subcarrier of a BS is allocated to the n^*th UE to reduce the possible impact on the availability of the other UEs. These three steps are iteratively executed until the available subcarrier set $\mathcal{F}$ becomes empty.

2) Power Allocation With Fixed Subcarrier Assignment and UE Association: Fixing the optimized subcarrier assignment and UE association in the first step, we limit $v^m_{s,n}$ to integer with fixed value. Thus, we can represent the optimization problem in (26) as

$$\min_{\boldsymbol{P}} \max_{n} \ \sum\nolimits_m \ln\left(1 - A^m_n\right) \tag{29}$$

$$\text{s.t.} \ \sum\nolimits_m P_{s,m} \le P^{max}_s, \quad \forall s \in \mathcal{B}, \tag{30a}$$

$$P_{s,m} \ge 0, \quad \forall s \in \mathcal{B}, \ \forall m \in \mathcal{M}. \tag{30b}$$

Following [38], we further convert this problem into the following optimization problem

$$\min_{\boldsymbol{v},\boldsymbol{p}} \ \zeta \tag{31}$$

$$\text{s.t.} \ \sum\nolimits_m P_{s,m} \le P^{max}_s, \quad \forall s \in \mathcal{B}, \tag{32a}$$

$$P_{s,m} \ge 0, \quad \forall s \in \mathcal{B}, \ \forall m \in \mathcal{M}, \tag{32b}$$

$$\sum\nolimits_m \ln\left(1 - A^m_n\right) \le \zeta, \quad \forall n \in \mathcal{N}. \tag{32c}$$

The above optimization problem can be solved by the Lagrangian dual method, where the corresponding Lagrangian is written as

$$\begin{aligned}\mathcal{L}(\boldsymbol{P};\boldsymbol{\alpha},\boldsymbol{\beta}) = \zeta &+ \sum_s \alpha_s \Big(\sum_m P_{s,m} - P^{max}_s\Big) \\ &+ \sum_n \beta_n \Big(\sum_m \ln(1 - A^m_n) - \zeta\Big),\end{aligned} \tag{33}$$

where $\boldsymbol{\alpha}$ ($\boldsymbol{\alpha} \ge 0$) is the Lagrange multiplier vector associated with constraint in (32a) and $\boldsymbol{\beta}$ ($\boldsymbol{\beta} \ge 0$) is the Lagrange multiplier vector associated with constraint in (32c). As such, the dual problem is given by

$$\max_{\boldsymbol{\alpha}\ge 0,\boldsymbol{\beta}\ge 0} \min_{\boldsymbol{P}} \mathcal{L}(\boldsymbol{P};\boldsymbol{\alpha},\boldsymbol{\beta}). \tag{34}$$

The above dual problem can be solved iteratively by decomposing it into two nested loops: the inner loop that minimizes over $\boldsymbol{P}$ with the given $\boldsymbol{\alpha}$ and $\boldsymbol{\beta}$, and the outer loop that is the master dual problem maximizing over $\boldsymbol{\alpha}$ and $\boldsymbol{\beta}$.

a) Solution to the inner loop: With the given $\boldsymbol{\alpha}$ and $\boldsymbol{\beta}$, $\min_{\boldsymbol{P}} \mathcal{L}(\boldsymbol{P};\boldsymbol{\alpha},\boldsymbol{\beta})$ is a standard concave form, and hence we apply the *Karush-Kuhn-Tucker* conditions to find the optimal solution. To solve the inner loop, we first derive the first-order derivatives as

$$\frac{\partial \mathcal{L}}{\partial P_{s,m}} = \alpha_s - \sum_n \beta_n \frac{1}{1 - A^m_n} \frac{\partial A^m_n}{\partial P_{s,m}}, \tag{35}$$

Note that A^m_n depends on $\mathcal{B}^m_n$ and I^m_n. If $\mathcal{B}^m_n = \emptyset$, we can directly obtain $\frac{\partial A^m_n}{\partial P_{s,m}} = 0$.

If $\mathcal{B}^m_n \ne \emptyset$ and $I^m_n = 0$, we derive

$$\begin{aligned}\frac{\partial A^m_n}{\partial P_{s,m}} &= \Omega_{\mathcal{B}^m_n} \sum_{s\in\mathcal{B}^m_n} \frac{e^{-\Xi_s \tau N_0}\Big(-\tau N_0 \Theta - \frac{\partial \Theta}{\partial \Xi_s}\Big)}{\Theta^2} \frac{\partial \Xi_s}{\partial P_{s,m}} \\ &= \frac{\Omega_{\mathcal{B}^m_n}}{P^2_{s,m} C_q d^{-\alpha_q}_{s,n}} \sum_{s\in\mathcal{B}^m_n} \frac{e^{-\Xi_s \tau N_0}}{\Theta^2}\Big(\tau N_0 \Theta - \upsilon_{k,s}\Big),\end{aligned} \tag{36}$$

where

$$\upsilon_{k,s} = \sum_{k\in\mathcal{B}^m_n/k,s} \ \prod_{k\in\mathcal{B}^m_n/s} \big(\Xi_k - \Xi_s\big). \tag{37}$$

If $B^m_n \ne \emptyset$ and $I^m_n \ne 0$, we have

$$\begin{aligned}\frac{\partial A^m_n}{\partial P_{s,m}} &= \frac{\partial \Xi_s \Omega_{\mathcal{B}}}{\partial P_{s,m}} \sum_{s\in\mathcal{B}^m_n} \sum_{j\in\mathcal{B}-\mathcal{B}^m_n} \Bigg(\frac{-\Upsilon}{\Theta^2_{\mathcal{B}^m_n/s}} \frac{\partial \Theta_{\mathcal{B}^m_n/s}}{\partial \Xi_s} \\ &\qquad + \frac{\partial \Upsilon}{\partial \Xi_s} \frac{1}{\Theta_{\mathcal{B}^m_n/s}}\Bigg) \\ &= \frac{\Omega_{\mathcal{B}}}{P^2_{s,m} C_q d^{-\alpha_q}_{s,n}} \sum_{s\in\mathcal{B}^m_n} \sum_{j\in\mathcal{B}-\mathcal{B}^m_n} \frac{\Upsilon \upsilon_{k,s}}{\Theta^2_{\mathcal{B}^m_n/s}} \\ &\quad - \frac{T_0(-N_0 - 1)\tau e^{-\theta_s N_0 \tau}}{\Theta_{\mathcal{B}-\mathcal{B}^m_n/j}\big(\Xi_j + \Xi_s \tau\big)^2 \Theta_{\mathcal{B}^m_n/s}},\end{aligned} \tag{38}$$

where

$$\Upsilon = \frac{e^{-\Xi_s N_0 \tau}}{\big(\Xi_j + \Xi_s \tau\big) \prod_{l\in\mathcal{B}-\mathcal{B}^m_n} \Big(\Xi_l - \Xi_j\Big)}. \tag{39}$$

By substituting (36) and (38) into (35) and setting $\frac{\partial L}{\partial P_{s,m}} = 0$, we derive the optimal power allocation $P^*_{s,m}$ as

$$P^*_{s,m} = \begin{cases} 0 & \text{if } |B^m_n| = 0 \\ \sqrt{\Im \Omega_{\mathcal{B}^m_n} \sum\limits_{s\in\mathcal{B}^m_n} \frac{e^{-\Xi_s \tau N_0}}{\Theta^2_{\mathcal{B}^m_n/s}} \left(\tau N_0 \Theta_{\mathcal{B}^m_n/s} - \upsilon_{k,s}\right)} & \text{if } B^m_n \ne \emptyset, I^m_n = 0 \\ \sqrt{\Im \Omega_{\mathcal{B}} \sum\limits_{s\in\mathcal{B}^m_n} \sum\limits_{j\in\mathcal{B}-\mathcal{B}^m_n} \left(\frac{\Upsilon \upsilon_{k,s}}{\Theta^2_{\mathcal{B}^m_n/s}} + \frac{(1+N_0)\tau e^{-\theta_s N_0 \tau}}{\Theta_{\mathcal{B}-\mathcal{B}^m_n/j}(\theta_j + \theta_s \tau)^2 \Theta_{\mathcal{B}^m_n/s}}\right)} & \text{if } B^m_n \ne \emptyset, I^m_n \ne 0 \end{cases} \tag{40}$$

where

$$\Im = \frac{1}{\alpha_s C_q d^{-\alpha_q}_{s,n}} \sum_n \frac{\beta_n}{1 - A^m_n}. \tag{41}$$

and $\Omega_{\mathcal{B}^m_n}$, $\Omega_{\mathcal{B}}$, $\Theta_{\mathcal{B}^m_n/j}$, $\Theta_{\mathcal{B}-\mathcal{B}^m_n/j}$, $\upsilon_{k,s}$ and Υ are given in (7) $\sim$ (10), (37) and (39).

Note that the local optimal solution ζ^* and local optimal availability $(A^m_n)^*$ can be obtained using $P^*_{s,m}$ in (40).

b) Solution to the outer loop: To find $\boldsymbol{\alpha}$ and $\boldsymbol{\beta}$ with the obtained $\boldsymbol{P}^*$ and ζ^* in the inner loop, we apply the subgradient method. By doing so, $\boldsymbol{\alpha}$ and $\boldsymbol{\beta}$ can be updated iteratively using

$$\alpha_s^{g+1} = \left[\alpha_s^g - \kappa\left(P_s^{max} - \sum_m P_{s,m}^*\right)\right]^+ \quad \forall s \in \mathcal{B}, \tag{42}$$

$$\beta_n^{g+1} = \left[\beta_n^g - \kappa\left(\zeta^* - \sum_m \ln(1-(A_n^m)^*)\right)\right]^+ \quad \forall n \in \mathcal{N}, \tag{43}$$

where $\kappa = \frac{0.1}{\sqrt{g}}$ is a diminishing step size, g is the iterative time, $[\cdot]^+$ denotes the updated $\boldsymbol{\alpha}$ and $\boldsymbol{\beta}$ needs to be non-negative.

The calculation process of the optimal power allocation $\boldsymbol{P}^*$ and the update process of $\boldsymbol{\alpha}$ and $\boldsymbol{\beta}$ are repeated until convergence, where the dual optimal is reached. Knowing that the inner loop is a convex problem, the duality gap is zero. The detailed procedures for solving the dual problem in (31) are illustrated in **Algorithm 2**.

Algorithm 2 Power Allocation Based on Lagrangian Dual Approach

Set $g = 0$, and initialize $\boldsymbol{\alpha}^g$, $\boldsymbol{\beta}^g$, and $\boldsymbol{P}$
repeat
  In prim domain, solve $\min_{\boldsymbol{P}} \mathcal{L}(\boldsymbol{P}; \boldsymbol{\alpha}, \boldsymbol{\beta})$ to obtain $\boldsymbol{P}^*$, ζ^* and $(A_n^m)^*$
  In dual domain, update the dual variable vector $\boldsymbol{\alpha}^{g+1}$ according to (42)
  In dual domain, update the dual variable vector $\boldsymbol{\beta}^{g+1}$ according to (43)
  $g = g + 1$
until *convergence*;

In TSOA, **Algorithm 2** is executed after **Algorithm 1**, we thus calculate the complexity of TSOA as $O(M^2S^2) + O(\mathcal{L})$, where S is the total number of BSs in $\mathcal{B}$, and $O(\mathcal{L})$ is the time complexity of **Algorithm 2**, which depends on the complexity of outer and inner loops. Due to the fact that **Algorithm 2** is a standard convex optimization, a fast convergence speed can be guaranteed for the subgradient method and power optimization based on KKT condition [20]. We thus can qualitatively conclude that $O(\mathcal{L})$ is low and acceptable. It also should be observed that algorithm 2 can only be executed after determining the subcarrier assignment and UE association, which means **Algorithm 1** and **Algorithm 2** can not be iteratively operated in TSOA. In the next section, we will design a GA based approach to iteratively update the subcarrier assignment and UE association, which will finally converge to the optimal solution. However, much more time complexity is required.

B. Joint Two-Step Optimization Based on Genetic Algorithm

In this section, we propose JTOA based on GA to achieve the interaction between the first step and the second step of TSOA. GA has already been widely used to tackle many real world NP-hard problems, such as BS placement optimization for LTE heterogeneous networks [39] or joint channel and power allocation for HetNets [40]. This bio-inspired algorithm imitates the natural evolution of biological organisms to provide a robust, near optimal solution for various problems.

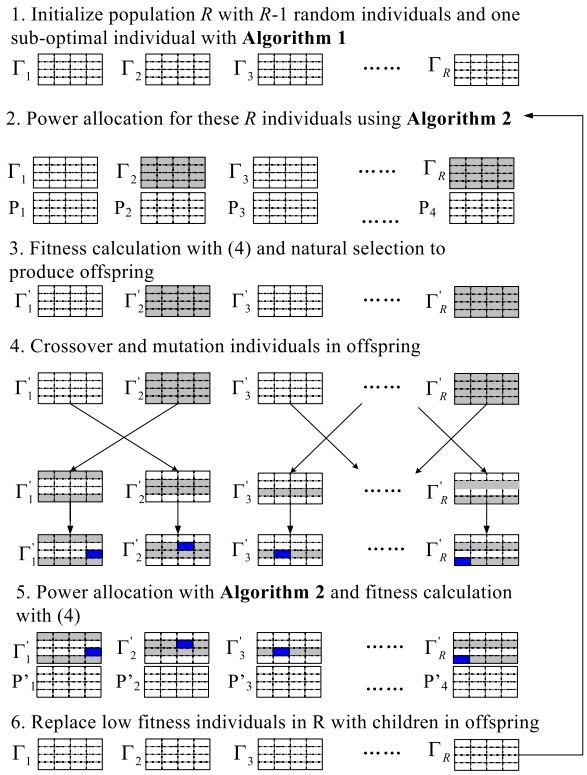

Fig. 3. Flowchart describing one iteration of the GA in solving the optimization problem.

In Fig. 3, the JTOA based on GA is illustrated in detail. The first operation is initialization. Initially, the GA generate R matrices to form the initial population set $\mathcal{R} = \{\Gamma^r\}_{r=1}^R$, where each matrix $\Gamma^r = \left[\gamma_{s,m}^r\right]_{S\times M}$ corresponds to a potential solution of the UE association and the subcarrier assignment. Each matrix element $\gamma_{s,m}^r \in \Gamma^r$ $(1 \le r \le R)$ denotes that the $\gamma_{s,m}^r$th UE is associated with the mth subcarrier of the sth BS $(0 \le \gamma_{s,m}^r \le N)$. Generally, the $\gamma_{s,m}^r$ in the initial population should be randomly generated to preserve the diversity of the population. However, considering that the solution obtained by our proposed heuristic algorithm in **Algorithm 1** is also a sub-optimal solution of the subcarrier assignment and UE association, we take the sub-optimal solution in **Algorithm 1** as a potential individual in the initial population. Thus, the initial population in our algorithm contains $R-1$ randomly generated individuals and one existing sub-optimal solution. By doing so, this initialization can converge much faster than that without using the sub-optimal solution in **Algorithm 1**, as validated by the simulation in Fig. 4b.

The initialized R individuals only describes the subcarrier assignment and UE association using $\mathcal{R} = \{\Gamma^r\}_{r=1}^R$. We then perform the power allocation for these R individuals using **Algorithm 2** based on the Lagrangian dual method in the second operation of Fig. 3.

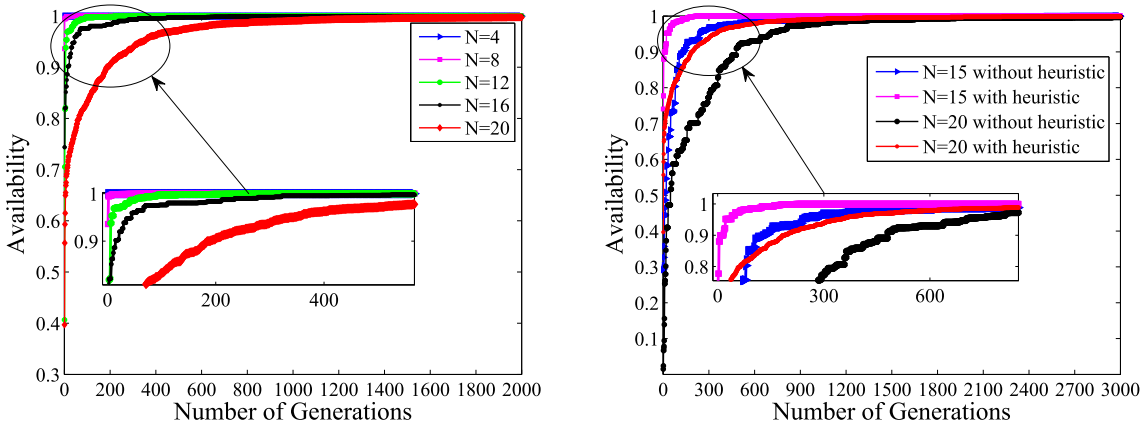

Fig. 4. (a) Convergence behavior with different number of UEs, (b) Convergence comparison with and without heuristic algorithm.

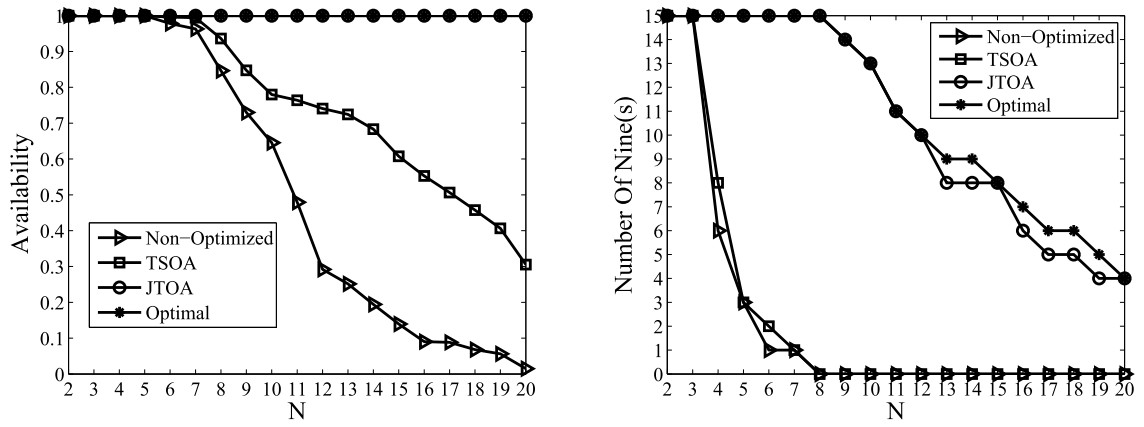

Fig. 5. Performance comparison with different number of UEs, (a) actual availability, (b) number of nines.

The third operation is the fitness value calculation and the natural selection. We calculate the fitness values (minimum UE availability) of all the individuals $\{\Gamma^r\}_{r=1}^R$ in population $\mathcal{R}$ as

$$f(r) = \min_n A_n, \quad \forall n \in \mathcal{N} \tag{44}$$

where A_n is calculated using (4). Each two individuals are selected using roulette wheel selection method [41], where the selection probability of each individual is given as

$$q_r = \frac{f(r)}{\sum_{r\in\mathcal{R}} f(r)}. \tag{45}$$

This selection is repeated until R individual are selected. These selected individuals are used to generate new populations with crossover and mutation operators.

The fourth operation is the crossover and the mutation. The conventional two-point crossover is performed to produce new solutions for two parent individuals in $\mathcal{R} = \{\Gamma^r\}_{r=1}^R$. We first randomly generate two crossover points, then each element between the two points are switched between two parent individuals to produce two child individuals. In the mutation operation, some elements in these two child individuals are randomly altered to diversify the population and pave the way towards optima. More specifically, each element of the matrix in $\mathcal{R} = \{\Gamma^r\}_{r=1}^R$ can be mutated or not decided by the predetermined mutation probability p_m. If a element $\gamma_{s,m}^r$ performs the mutation, a random integer value x between 1 and N will be chosen to replace the original value ($\gamma_{s,m}^r = x$).

The sixth operation is the replacement based on an elitist model, which is used to update a certain number of individuals in the old population with the new generated individuals. Since the UE association and subcarrier assignment described by individuals have been altered during third and fourth operation, we need to calculate the fitness value of the new generated individuals using (44) in the fifth operation, then the parent individuals with the low fitness value will be replaced by the new generated individuals with higher fitness value in the next generation in the sixth operation. This population evolution operations will repeat until convergence, where the convergence is defined when the maximum fitness value remains constant for a fixed number of successive iterations [42].

The JTOA of the UE association and subcarrier assignment, and the power allocation based on GA is described in **Algorithm 3**, where G is the given number of generations,

R is the population size, p_c is the crossover probability, and p_m is the mutation probability. Due to the fact the Lagrangian dual method is applied to evaluate each individual in each population, the time complexity of solving this JTOA is $O(GR(O(\mathcal{L}) + R))$, which showcases the higher implementation complexity is required to obtain a better solution compared with that of TSOA.

Algorithm 3 JTOA

set $g = 1$
Generate initiation population with $R - 1$ randomly generated individuals and 1 individual by **Algorithm 1**
Calculate fitness value for each individual in $\mathcal{R}$ using **Algorithm 2**
repeat
  for $i = 1$ **to** $R/2$ **do**
    Select two parents p_1 and p_2 from $\mathcal{R}$ using roulette wheel selection method
    $r_{2*i-1} = p_1$ and $r_{2*i} = p_2$
    Cross r_{2*i-1} and r_{2*i} using two-point crossover strategy with probability p_c, and produce two children r'_{2*i-1} and r'_{2*i}
    Mutate r'_{2*i-1} and r'_{2*i} using mutation strategy with probability p_m
    $\mathcal{R}' = \mathcal{R}' \cup \{r'_{2*i-1}, r'_{2*i}\}$
    Calculate fitness value for each individual in $\mathcal{R}'$ using **Algorithm 2**
  end
  Replace the individuals with low fitness values in population $\mathcal{R}$ with the children in offspring $\mathcal{R}'$
until *convergence*;
Return the fittest individual in $\mathcal{R}$

V. Numerical Results

In this section, we provide numerical results to illustrate the performance of our proposed algorithm. We consider CoMP and CA-enabled HetNets consisting of 2 tiers (marco and pico) with 2 bands (800MHz and 2.5GHz), where each band has a bandwidth of 10MHz. The set-up is a circle area with size $(\pi 500^2)$ m^2, where the macro BS is located at the center, the pico BSs and UEs are randomly distributed in this circle area. The details of parameters are summarized in Table I unless otherwise specified. All the results are obtained by averaging 100 random simulations, and the obtained availability is the minimum availability among all UEs.

Fig. 4a plots the convergence behavior of our proposed JTOA with different number of UEs with $M = 20$, 9 Pico BSs and 1 Marco BS, where the initial population is a solution generated by proposed heuristic algorithm in **Algorithm 1**. Fig. 4b plots the convergence behavior of JTOA, where the initial population is a solution generated by proposed heuristic algorithm in **Algorithm 1** or random generated population. In Fig. 4a, we see that our proposed algorithm converges after approximately 1000 number of generations for various number of UEs. However, in Fig. 4b, we notice that our proposed algorithm converges approximately after 1500 generations if the initial population is not generated by the sub-optimal solution in **Algorithm 1**. This reveals that applying **Algorithm 1** for initial population generation can speed up convergence. In both figures, we observe that the converge speed can be substantially increased with decreasing number of UEs in HetNets.

TABLE I
Simulation Parameters

Parameter	Value
The number of macro BS	1
The number of pico BS	$1 \sim 9$
The number of UEs	$2 \sim 20$
Maximum transmit power of macro BS	46dBm (40W)
Maximum transmit power of pico BS	30dBm (1W)
800MHz band's wavelength μ_1	0.375m
2.5GHz band's wavelength μ_2	0.125m
800MHz band's path loss exponent α_1	3
2.5GHz band's path loss exponent α_2	4
The number of subcarriers in each band	10
Noise PSD	-174dBm
SINR threshold τ	1
Population size	20
Crossover probability	0.95
Mutation probability	0.005
Maximum generation	3000

TABLE II
Optimized Availability Value

Tech. \ N	4	8	12	16	20
CA	10 nines	7 nines	5 nines	3 nines	3 nines
CA & CoMP	15 nines	15 nines	10 nines	6 nines	4 nines

In Table II, we also present the optimized availability based on JTOA for various number of UEs with and without CoMP in HetNets. We see that with the interference coordination at each path, the optimized availability is always higher than that without CoMP, which can be contributed to the single path gain obtained via CoMP. More importantly, with higher number of UEs, the benefits of CoMP in achieving high availability in HetNets become less obvious, which is due to the reduced number of paths for each UE.

Fig. 5 compares the optimized UE availability based on our proposed JTOA with that based on TSOA, and the non-optimized UE availability, and the optima with $M = 20$, 9 Pico BSs and 1 Marco BS. Here, the optima is obtained by searching all feasible subcarrier allocations with brute force approach. Note that Fig. 5a plots the actual availability, and Fig. 5b plots the corresponding number of nines. We first observe that the availability decreases with increasing the number of UEs. This can be explained by the fact that the transmit power allocated to the UE decreases and the interference from the same subcarrier at other BSs increases with increasing the number of UEs. More importantly, the optimized UE availability based on JTOA outperforms that based on TSOA, and the non-optimized UE availability, and closely approaches the performance of the optima obtained by brute force approach, which showcases the effective of our proposed JTOA.

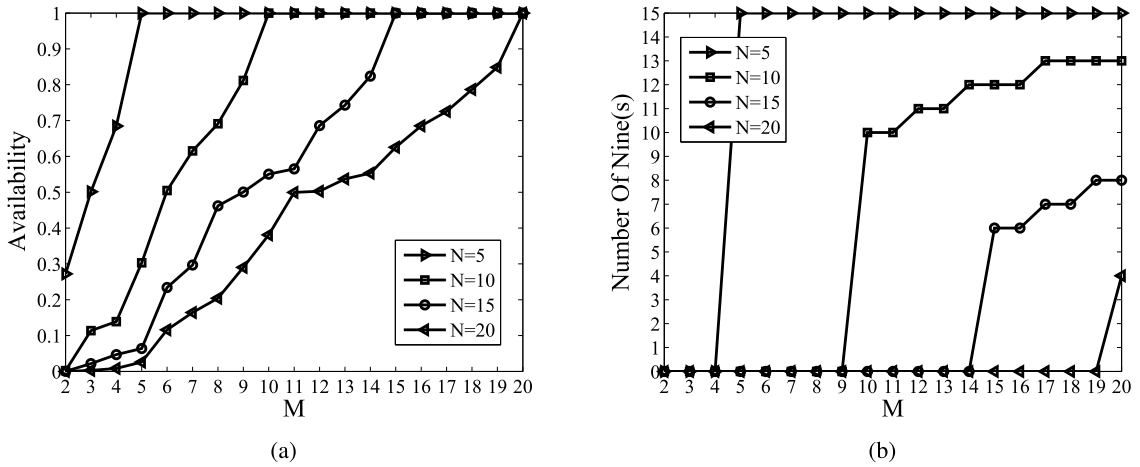

Fig. 6. Availability with different number of subcarriers, (a) actual availability, (b) number of nines.

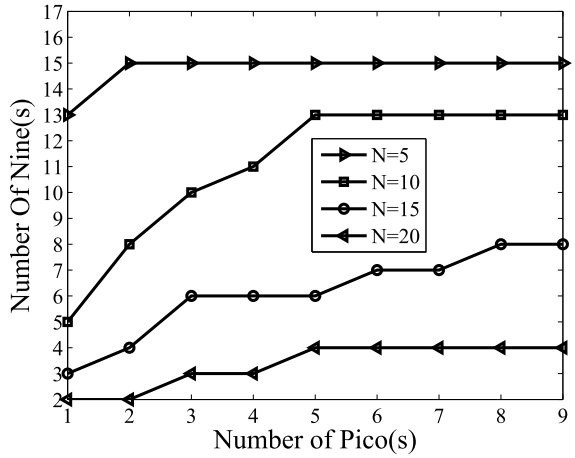

Fig. 7. Availability with different number of Pico BSs.

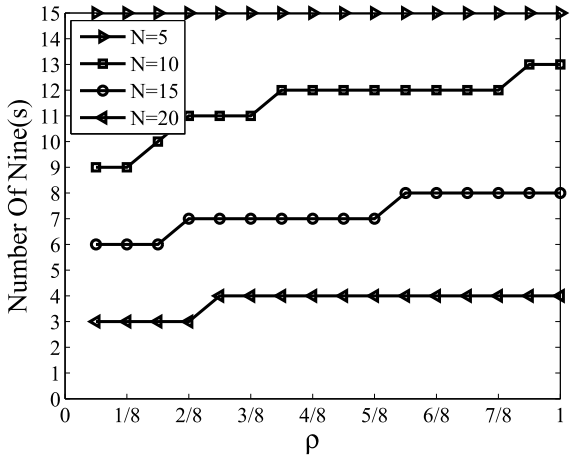

Fig. 8. Availability with diferent allocated power ratio.

Fig. 6 plots the availability versus the number of subcarriers per BS M with 9 Pico BSs and 1 Marco BS, where Fig. 6a plots the actual availability and Fig. 6b plots the corresponding number of nines. We can see that the availability increases with increasing the number of available subcarriers. This can be explained by the fact that interference decreases with the increasing the number of subcarriers, thus the single path availability is improved. This can also be contributed to the fact that increasing the number subcarriers also increases the potential gain from the spectral diversity. We find that more subcarriers are needed to achieve the same availability with more UEs. In order to achieve a minimum availability of 6 nines, we need at least 15 subcarriers per BS for 15 random deployed UEs.

Fig. 7 plots the availability versus the number of Pico BSs with $M = 20$. We can see that the availability increases with increasing the number of Pico BSs. This is because increasing the number of Pico BSs increases the number of paths can be connected for each UE, and decreases the co-channel interference in the same subcarrier. However, we observe that availability can not be further increased when the number of Pico BSs is larger than 8. This indicates that increasing the number of Pico BSs can not constantly increase the UE availability.

Fig. 8 plots the availability versus the BS allocated power ratio ρ with $M = 20$, 9 Pico BSs and 1 Marco BS, where ρ is the maximum BS allocated power divided by the maximum BS transmit power. It is shown that the availability increases with increasing ρ. For the number of UEs is small $N = 5$, 10, or 15, 6 nines availability can be achieved with very low allocated power ratio $\rho = 1/16$, whereas for large number of UEs $N = 20$, 6 nines availability can not be achieved even with full power allowance $\rho = 1$. This indicates that increasing the BS power allocation ratio can not always guarantee substantial improvement in the availability of HetNets.

VI. Conclusions

In this paper, we have presented the theoretical model and optimization algorithms to achieve high availability in CoMP and CA-enabled HetNets. We have derived a closed-form expression for the availability of random UEs in a CoMP and CA-enabled HetNets. We have formulated an optimization problems to maximize the minimum availability under the BS transmit power constraint. To solve the optimization problem,

we have proposed the TSOA, where the subcarrier assignment and UE association solution is obtained via heuristic algorithm, and power allocation solution is obtained via Lagrangian dual based method. Moreover, we have proposed JTOA based on GA to achieve the interaction between the first step and the second step. Numerical results show that our proposed JTOA is effective in achieving ultra-high availability. The high availability requirement in 5G applications, such as haptic communications, can be achieved via multiple connectivity with CA and CoMP. However, when the number of UEs is small, increasing the number of Pico BSs and the power allocation ratio can not constantly increase the UE availability.

REFERENCES

[1] J. Jia, Y. Deng, J. Chen, H. Aghvami, A. Nallanathan, and X. Wang, "Optimizing availability in CoMP and CA-enabled HetNets," in *Proc. IEEE ICC*, May 2017, pp. 1–6.

[2] Gartner. (2015). *Gartner Says 6.4 Billion Connected 'Things' Will be in Use in 2016, up 30 Percent From 2015*. [Online]. Available: http://www.gartner.com/newsroom/id/3165317

[3] E. Steinbach *et al.*, "Haptic communication," *Proc. IEEE*, vol. 100, no. 4, pp. 937–956, Apr. 2012.

[4] M. Jammal, A. Kanso, and A. Shami, "High availability-aware optimization digest for applications deployment in cloud," in *Proc. IEEE ICC*, Jun. 2015, pp. 6822–6828.

[5] Z. M. Fadlullah, M. M. Fouda, N. Kato, A. Takeuchi, N. Iwasaki, and Y. Nozaki, "Toward intelligent machine-to-machine communications in smart grid," *IEEE Commun. Mag.*, vol. 49, no. 4, pp. 60–65, Apr. 2011.

[6] X. Ge, H. Cheng, G. Mao, Y. Yang, and S. Tu, "Vehicular communications for 5G cooperative small-cell networks," *IEEE Trans. Veh. Commun.*, vol. 65, no. 10, pp. 7882–7994, Oct. 2016.

[7] A. Frotzscher *et al.*, "Requirements and current solutions of wireless communication in industrial automation," in *Proc. IEEE ICC Workshops*, Jun. 2014, pp. 67–72.

[8] TR ETSI. 102 889-2 v1. 1.1. *Electromagnetic Compatibility and Radio Spectrum Matters (ERM)*. [Online]. Available: http://www.etsi.org/technologiesclusters/technologies/emc.

[9] G. P. Fettweis, "The tactile internet: Applications and challenges," *IEEE Veh. Technol. Mag.*, vol. 9, no. 1, pp. 64–70, Mar. 2014.

[10] X. Ge, J. Ye, Y. Yang, and Q. Li, "User mobility evaluation for 5G small cell networks based on individual mobility model," *IEEE J. Sel. Areas Commun.*, vol. 34, no. 3, pp. 528–541, Mar. 2016.

[11] J. Pukite and P. Pukite, *Modeling for Reliability Analysis: Markov Modeling for Reliability, Maintainability, Safety, and Supportability*. Hoboken, NJ, USA: Wiley, Jun. 1998.

[12] D. Öhmann, M. Simsek, and G. P. Fettweis, "Achieving high availability in wireless networks by an optimal number of Rayleigh-fading links," in *Proc. IEEE Globecom Workshops (GC Wkshps)*, Dec. 2014, pp. 1402–1407.

[13] D. Ohmann, W. Teske, and G. P. Fettweis, "Combining Nakagami-*m* fading links for high availability in wireless networks," in *Proc. IEEE VTC*, 2015, pp. 1–6.

[14] Z. Rui, W. Jibo, and V. C. M. Leung, "Outage probability of composite microscopic and macroscopic diversity over correlated shadowed fading channels," *China Commun.*, vol. 10, no. 11, pp. 129–142, Nov. 2013.

[15] N. A. Johansson, Y. P. E. Wang, E. Eriksson, and M. Hessler, "Radio access for ultra-reliable and low-latency 5G communications," in *Proc. IEEE ICC Workshop*, Jun. 2015, pp. 1184–1189.

[16] G. Pocovi, B. Soret, M. Lauridsen, K. I. Pedersen, and P. Mogensen, "Signal quality outage analysis for ultra-reliable communications in cellular networks," in *Proc. IEEE Glebecom Workshops*, Dec. 2015, pp. 1–6.

[17] X. Ge, K. Huang, C. X. Wang, X. Hong, and X. Yang, "Capacity analysis of a multi-cell multi-antenna cooperative cellular network with co-channel interference," *IEEE Trans. Wireless Commun.*, vol. 10, no. 10, pp. 3298–3309, Oct. 2011.

[18] D. Oehmann, A. Awada, I. Viering, M. Simsek, and G. P. Fettweis, "SINR model with best server association for high availability studies of wireless networks," *IEEE Wireless Commun. Lett.*, vol. 5, no. 1, pp. 60–63, Feb. 2016.

[19] H. Lee, S. Vahid, and K. Moessner, "A survey of radio resource management for spectrum aggregation in LTE-advanced," *IEEE Commun. Surveys Tuts.*, vol. 16, no. 2, pp. 745–760, 2nd Quart., 2014.

[20] G. Yu, Q. Chen, R. Yin, H. Zhang, and G. Y. Li, "Joint downlink and uplink resource allocation for energy-efficient carrier aggregation," *IEEE Trans. Wireless Commun.*, vol. 14, no. 6, pp. 3207–3218, Jun. 2015.

[21] J. Jia, Y. Deng, S. Ping, H. Aghvami, and A. Nallanathan, "High availability optimization in heterogeneous cellular networks," in *Proc. IEEE GLOBECOM*, Dec. 2016, pp. 1–6.

[22] X. Lin, J. G. Andrews, R. Ratasuk, B. Mondal, and A. Ghosh, "Carrier aggregation in heterogeneous cellular networks," in *Proc. IEEE Int. Conf. Commun. (ICC)*, Jun. 2013, pp. 5199–5203.

[23] "Coordinated multipoint operation for LTE physical layer aspects (release 11)," Sophia-Antipolis, France, 3GPP, Tech. Rep. 36.819, V11.1.0, 2011.

[24] Y. Cheng, M. Pesavento, and A. Philipp, "Joint network optimization and downlink beamforming for comp transmissions using mixed integer conic programming," *IEEE Trans. Signal Process.*, vol. 61, no. 16, pp. 3972–3987, Aug. 2013.

[25] Z. Xu, C. Yang, G. Y. Li, Y. Liu, and S. Xu, "Energy-efficient CoMP precoding in heterogeneous networks," *IEEE Trans. Signal Process.*, vol. 62, no. 4, pp. 1005–1017, Feb. 2014.

[26] M. Hong, R. Sun, H. Baligh, and Z. Q. Luo, "Joint base station clustering and beamformer design for partial coordinated transmission in heterogeneous networks," *IEEE J. Sel. Areas Commun.*, vol. 31, no. 2, pp. 226–240, Feb. 2013.

[27] P. Xia, C.-H. Liu, and J. G. Andrews, "Downlink coordinated multi-point with overhead modeling in heterogeneous cellular networks," *IEEE Trans. Wireless Commun.*, vol. 12, no. 8, pp. 4025–4037, Aug. 2013.

[28] L. Liu, V. Garcia, L. Tian, Z. Pan, and J. Shi, "Joint clustering and inter-cell resource allocation for CoMP in ultra dense cellular networks," in *Proc. IEEE ICC*, Jun. 2015, pp. 2560–2564.

[29] S. Han, B.-H. Soong, and Q. D. La, "Subcarrier allocation in multi-cell OFDMA wireless networks with non-coherent base station cooperation and controllable fairness," in *Proc. 23rd IEEE PIMRC*, Sep. 2012, pp. 524–529.

[30] X. Wang, F.-C. Zheng, P. Zhu, and X. You, "Energy-efficient resource allocation in coordinated downlink multicell OFDMA systems," *IEEE Trans. Veh. Technol.*, vol. 65, no. 3, pp. 1395–1408, Mar. 2015.

[31] J. G. Andrews, F. Baccelli, and R. K. Ganti, "A tractable approach to coverage and rate in cellular networks," *IEEE Trans. Commun.*, vol. 59, no. 11, pp. 3122–3134, Nov. 2011.

[32] H. S. Dhillon, R. K. Ganti, F. Baccelli, and J. G. Andrews, "Modeling and analysis of K-tier downlink heterogeneous cellular networks," *IEEE J. Sel. Areas Commun.*, vol. 30, no. 3, pp. 550–560, Apr. 2012.

[33] D. Lee *et al.*, "Coordinated multipoint transmission and reception in LTE-advanced: Deployment scenarios and operational challenges," *IEEE Commun. Mag.*, vol. 50, no. 2, pp. 148–155, Feb. 2012.

[34] V. Garcia, Y. Zhou, and J. Shi, "Coordinated multipoint transmission in dense cellular networks with user-centric adaptive clustering," *IEEE Trans. Wireless Commun.*, vol. 13, no. 8, pp. 4297–4308, Aug. 2014.

[35] M. Balázs. (2005). *Sum of Independent Exponentials*. [Online]. Available: http://www.math.bme.hu/balazs/sumexp.pdf

[36] K. D. Lee and V. C. M. Leung, "Fair allocation of subcarrier and power in an OFDMA wireless mesh network," *IEEE J. Sel. Areas Commun.*, vol. 24, no. 11, pp. 2051–2060, Nov. 2006.

[37] D. Bertsimas, O. Nohadani, and K. M. Teo, "Nonconvex robust optimization for problems with constraints," *Informs J. Comput.*, vol. 22, no. 1, pp. 44–58, Aug. 2010.

[38] M. Rugelj, U. Sedlar, M. Volk, J. Sterle, M. Hajdinjak, and A. Kos, "Novel cross-layer QoE-aware radio resource allocation algorithms in multiuser OFDMA systems," *IEEE Trans. Commun.*, vol. 62, no. 9, pp. 3196–3208, Sep. 2014.

[39] S. Lee, S. Lee, K. Kim, and Y. H. Kim, "Base station placement algorithm for large-scale LTE heterogeneous networks," *PLoS ONE*, vol. 10, no. 10, pp. 0139190, Oct. 2015.

[40] K. Nakamura, T. Tashiro, K. Yamamoto, and K. Ohno, "Transmit power control and channel assignment for femto cells in HetNet systems using genetic algorithm," in *Proc. 26th IEEE PIMRC*, Aug./Sep. 2015, pp. 1669–1674.

[41] D. E. Goldberg, *Genetic Algorithms*. Uttar Pradesh, India: Pearson Education India, 2006.

[42] H. Ghazzai, E. Yaacoub, M.-S. Alouini, and A. Abu-Dayya, "Optimized smart grid energy procurement for LTE networks using evolutionary algorithms," *IEEE Trans. Veh. Technol.*, vol. 63, no. 9, pp. 4508–4519, Nov. 2014.

Jie Jia received the Ph.D. degree in computer science and technology from Northeastern University in 2009. In 2016, she was a Visiting Research Associate with the King's College London. She is currently an Associate Professor with Northeastern University, China. She has authored over 100 technical papers on various aspects of wireless networks. Her current research mainly focuses on HetNets, IoT, and cognitive radio networks. She is a member of various international societies including the China Computer Federation.

Yansha Deng (S'13–M'16) received the Ph.D. degree in electrical engineering from the Queen Mary University of London, U.K., 2015. She is currently the Post-Doctoral Research Fellow with the Department of Informatics, King's College London, U.K. Her research interests include massive MIMO, HetNets, molecular communication, cognitive radio, cooperative networks, and physical layer security. She received the Best Paper Award at the ICC 2016. She has also served as the TPC Member for many IEEE conferences, such as the IEEE GLOBECOM and the ICC. She is currently an Editor of the IEEE COMMUNICATIONS LETTERS.

Jian Chen received the Ph.D. degree in computer science and technology from Northeastern University in 2010. In 2016, he was a Visiting Research Associate with the King's College London. He is currently an Associate Professor with Northeastern University, and as a Senior Software Engineer with Neusoft Corporation. His research interests include D2D communication, location technology, network management, signal, and image processing.

Abdol-Hamid Aghvami (M'89–SM'91–F'05) joined the academic staff, King's College London, in 1984. He was promoted to a Reader and to a Professor of Telecommunications Engineering in 1989 and 1993, respectively. He is the Founder of the Center for Telecommunications Research, King's College London, where he was the Director of the Center from 1994 to 2014. He is currently a Professor of Telecommunications Engineering with the King's College London.

He was a Visiting Professor with the NTT Radio Communication Systems Laboratories in 1990. He was a Senior Research Fellow with the BT Laboratories from 1998 to 1999, and was an Executive Advisor with Wireless Facilities Inc., USA, from 1996 to 2002. He is also the Chairman of the Advanced Wireless Technology Group Ltd. He is also the Managing Director of Wireless Multimedia Communications Ltd., his own consultancy company. He carries out consulting work on digital radio communications systems for British and International companies. He has authored over 560 technical journal and conference papers, filed 30 patents and given invited talks and courses the world over on various aspects of mobile radio communications.

He also leads an active research team involved in numerous mobile and personal communications projects for fourth and fifth generation networks, which are supported both by government and industry. He was a member of the Board of Governors of the IEEE Communications Society from 2001 to 2003, was a Distinguished Lecturer of the IEEE Communications Society from 2004 to 2007, and has been member, Chairman, and Vice-Chairman of the technical program and organizing committees of a large number of international conferences. He is also the Founder of the International Symposium on Personal Indoor and Mobile Radio Communications, a major yearly conference attracting some 1,000 attendees.

Dr. Aghvami was a recipient of the IEEE Technical Committee on Personal Communications Recognition Award in 2005 for his outstanding technical contributions to the communications field, and for his service to the scientific and engineering communities. He is a Fellow of the Royal Academy of Engineering and Fellow of the IET. He received a Fellowship of the Wireless World Research Forum in recognition of his personal contributions to the wireless world in 2009 and for his research achievements as Director with the Center for Telecommunications Research at King's College London.

Arumugam Nallanathan (S'97–M'00–SM'05–F'17) is currently a Professor of Wireless Communications with the Department of Informatics, King's College London (University of London). He served as the Head of Graduate Studies with the School of Natural and Mathematical Sciences, King's College London, from 2011 to 2012. He was an Assistant Professor with the Department of Electrical and Computer Engineering, National University of Singapore, from 2000 to 2007. His research interests include 5G wireless networks, Internet of things, and molecular communications. He has authored over 300 technical papers in scientific journals and international conferences. He was a co-recipient of the Best Paper Award presented at the IEEE International Conference on Communications 2016 and the IEEE International Conference on Ultra-Wideband 2007. He is currently an IEEE Distinguished Lecturer. He has been selected as a Web of Science Highly Cited Researcher in 2016.

He is currently an Editor of the IEEE TRANSACTIONS ON COMMUNICATIONS and the IEEE TRANSACTIONS ON VEHICULAR TECHNOLOGY. He was an Editor of the IEEE TRANSACTIONS ON WIRELESS COMMUNICATIONS from 2006 to 2011, the IEEE WIRELESS COMMUNICATIONS LETTERS and the IEEE SIGNAL PROCESSING LETTERS. He served as the Chair of the Signal Processing and the Communication Electronics Technical Committee of IEEE Communications Society and the Technical Program Chair and member of the Technical Program Committees in numerous IEEE conferences. He received the IEEE Communications Society SPCE Outstanding Service Award 2012 and the IEEE Communications Society RCC Outstanding Service Award 2014.